



OPEN ACCESS

EDITED BY

Qiang Li,
Chinese Academy of Geological Sciences,
China

REVIEWED BY

Yanlin Zhao,
Hunan University of Science and
Technology, China
Tianliang Zheng,
Chengdu University of Technology, China

*CORRESPONDENCE

Jianyao Chen
✉ chenjiyao@mail.sysu.edu.cn
Lei Gao
✉ 416581541@qq.com

SPECIALTY SECTION

This article was submitted to
Terrestrial Microbiology,
a section of the journal
Frontiers in Microbiology

RECEIVED 26 September 2022

ACCEPTED 15 December 2022

PUBLISHED 17 January 2023

CITATION

Liang Z, Li S, Wang Z, Li R, Yang Z, Chen J,
Gao L and Sun Y (2023) Microbial
community structure characteristics
among different karst aquifer systems, and
its potential role in modifying hydraulic
properties of karst aquifers.
Front. Microbiol. 13:1054295.
doi: 10.3389/fmicb.2022.1054295

COPYRIGHT

© 2023 Liang, Li, Wang, Li, Yang, Chen,
Gao and Sun. This is an open-access article
distributed under the terms of the [Creative
Commons Attribution License \(CC BY\)](https://creativecommons.org/licenses/by/4.0/). The
use, distribution or reproduction in other
forums is permitted, provided the original
author(s) and the copyright owner(s) are
credited and that the original publication in
this journal is cited, in accordance with
accepted academic practice. No use,
distribution or reproduction is permitted
which does not comply with these terms.

Microbial community structure characteristics among different karst aquifer systems, and its potential role in modifying hydraulic properties of karst aquifers

Zuobing Liang^{1,2}, Shaoheng Li¹, Zhuowei Wang³, Rui Li¹,
Zhigang Yang⁴, Jianyao Chen^{1*}, Lei Gao^{5*} and Yuchuan Sun⁶

¹School of Geography and Planning, Sun Yat-sen University, Guangzhou, China, ²Key Laboratory of Groundwater Sciences and Engineering, Ministry of Natural Resources, Shijiazhuang, China, ³China Institute of Water Resources and Hydropower Research, Beijing, China, ⁴Department of Hydraulic Engineering, Tsinghua University, Beijing, China, ⁵South China Botanical Garden, Chinese Academy of Sciences, Guangzhou, China, ⁶Chongqing Key Laboratory of Karst Environment, School of Geographical Sciences, Southwest University, Chongqing, China

Little is known about how microbial activity affects the hydraulic properties of karst aquifers. To explore the potential impacts of microbial activity on the hydraulic properties of karst aquifers, microbiological analysis, heat tracer, isotope (dissolved inorganic carbon isotope, $\delta^{13}\text{C}_{\text{DIC}}$) and aqueous geochemical analyses were conducted at six monitoring wells in Northern Guangdong Province, China. Greater hydraulic conductivity corresponded to a low temperature gradient to an extent; the temperature gradient in karst groundwater aquifers can reflect the degree of dissolution. Higher HCO_3^- concentrations coupled with lower d-excess and pH values at B2 and B6 reflect potential microbial activity (e.g., *Sulfuricurvum kujiense*) causing carbonate dissolution. Microbial activity or the input of anthropogenic acids, as evidenced by significantly more positive $\delta^{13}\text{C}_{\text{DIC}}$ values, potentially affect carbonate dissolution in deep karst aquifers, which eventually alters hydraulic properties of karst aquifer. However, more direct evidence is needed to quantify the effects of microbial activity on carbonate dissolution in karst aquifers.

KEYWORDS

karst aquifer, subsurface microbiology, heat tracer, isotopes, hydraulic properties

1. Introduction

Karst regions cover 7~12% of the Earth's continental area, and their aquifers are a source of drinking water for almost one quarter of the global population (Ford and Williams, 2007). However, karst aquifers have complex characteristics that make them very different from other aquifers, because they are self-developing, dissolved bedrock

constituents are transported through and out of the system (Ford and Williams, 2007), and this unique property of the aquifer results in difficulty developing and utilizing karst groundwater (Goldscheider and Drew, 2007).

Karst aquifers can be modified by external factors, such as climate change (Loáiciga, 2009), which alter the flux of meteoric water into the system and change the pressure or temperature imparted by vertically migrating fluids and internal processes (Corbella and Ibáñez, 2003), like chemical reactions (Loáiciga, 2009) and microbial activity (Engel et al., 2004a,b). In addition, mine water produced by mining activities also accelerate the dissolution rate of rocks in karst aquifers (Zhao et al., 2020; Liu et al., 2022), and seepage-damage effect in fractured rocks of karst aquifers may also produce great influences on the conductivity of karst aquifer (Zhao et al., 2021). More studies of microbial control of karst processes have focused on the sulfidic, saline water zones of karst aquifers (Engel and Randall, 2011; Gray and Engel, 2013). However, few reports have been focused on carbonate dissolution in freshwater aquifers. Lianjiang River Basin (LRB) is located in the north of Guangdong Province, China, characterized by high spatial hydrogeological heterogeneity. The LR system belongs to the trellis drainage, extending from the northwest to the southeast of the drainage basin. In the northwest of the LRB, karst aquifers have low permeability and low water richness, fissures are not developed; in the southeast of the drainage basin, karst aquifers have high permeability, joints and fissures are relatively developed, and dissolution is obvious.

In the present study, we determined the $n\sim$ Alkanes biomarkers, groundwater temperature, dissolved inorganic carbon isotope ($\delta^{13}\text{C}_{\text{DIC}}$), microbial community and hydrochemical characteristics of groundwater from the LRB to elaborate the following objectives: (1) ascertaining the structures of microbial communities in different karst aquifers; (2) exploring the effects of biogeochemical processes in modifying hydraulic properties.

2. Materials and methods

2.1. Well selection and geochemical analyses

Six monitoring wells are located in the Lianjiang River basin: B1 and B2 are upstream, B3–B5 are in midstream, and B6 is downstream (Figure 1). B1 is in an area of Cretaceous Nanxion calcareous mudstone; B2 is in an area of Devonian (Baqi/Liujiang) carbonate; B3 is in an area of Devonian Rongxian carbonate; B4 and B5 are in an area of Carboniferous Shidengzi carbonate; and B6 is in an area of Devonian Tianziling carbonate. More information about the lithology of selected boreholes was seen in attachment files (Supplementary Figure S1; Supplementary Table S1).

Groundwater from the sampling wells was sampled after pumping. Parameters, including pH, dissolved oxygen (DO) concentration, electrical conductivity (EC), and temperature (T) were quantified with a portable water quality analyzer (Horiba D-24, Japan). The concentration of bicarbonate (HCO_3^-) was

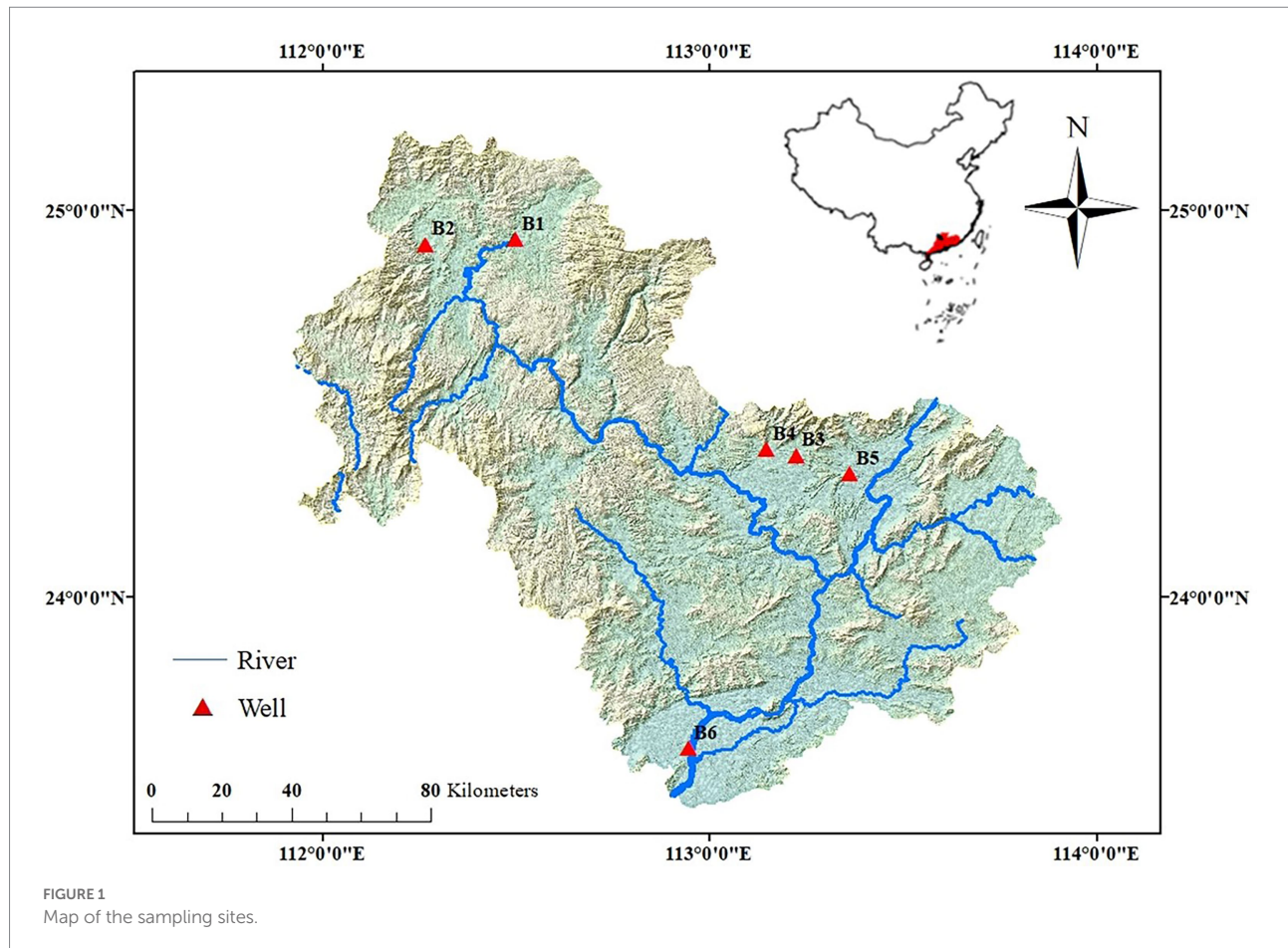
measured *in situ* using the titration kit (Merck, Germany). Water samples were filtered after sampling using a 0.22 μm cellulose acetate filter and then stored in precleaned polypropylene bottles. Major anions (Cl^- , NO_3^- , and SO_4^{2-}) of filtered water samples were determined *via* ion chromatography (ICS 900, Dionex, United States). One aliquot of filtered water samples was acidified to $\text{pH} < 2$ with ultra-purified HNO_3 for analyses of major cations (K^+ , Na^+ , Ca^{2+} , and Mg^{2+}) measurements using inductively coupled plasma-atomic emission spectrometry (ICP-AES, IRIS-HR, United States). The $\delta^{18}\text{O}$ of ground water values were analyzed using a high-precision laser isotope analyzer (Picarro L2130-i Analyzer) with the measurement accuracy of 0.02%, and measurements were reported relative to the V-SMOW standard. $\delta^{13}\text{C}_{\text{DIC}}$ values were analyzed using a MAT-253 mass spectrometer coupled with a Gas Bench II automated device with analytical precision of $\pm 0.15\%$. The results are expressed as $\delta^{13}\text{C}_{\text{DIC}}$ (‰) with respect to the Vienna Pee Dee Belemnite (V-PDB) standard. Aqueous geochemical analyses and computational modeling provided saturation conditions for aquifer minerals, specifically calcite, dolomite and gypsum. The saturation index (SI) of a mineral is defined as $\log(\text{IAP}/\text{Ksp})$, where IAP is the ion activity product and Ksp is a mineral thermodynamic equilibrium constant. A positive SI value indicates that precipitation with respect to a mineral is thermodynamically possible, whereas negative SI values indicate dissolution. A SI of 0 ± 0.5 indicates a mineral is at equilibrium within the solution (Gray and Engel, 2013). Deuterium excess (d-excess) is a second-order isotope parameter that is a function of the isotopic composition of oxygen and hydrogen in water, as defined by the Dansgaard's equation: $\text{d-excess} = \delta^2\text{H} - 8 \times \delta^{18}\text{O}$ (Dansgaard, 1964).

2.2. Groundwater temperature data collection

The temperature–depth (TD) profiles of the six wells were determined using a COMPACT-TD logger (JFE Advantech, Japan), which simultaneously records water temperature and depth automatically; this equipment has a temperature resolution of 0.001°C and depth resolution of 0.008 m for every monitoring depth. Measurements were repeated to ensure that the equipment reached equilibrium with the surrounding environment (Li et al., 2019b). ‘Temperature-depth’ profile in the subsurface can be divided into the surficial zone and the geothermal zone (Parsons, 1970), and within the surficial zone temperature is influenced by seasonal heating and cooling of the land surface. Temperature profiles in the surficial zone potentially provide information about seasonal recharge/discharge events from precipitation and interchange with surface water (Anderson, 2005).

2.3. Microbiological analysis

For the microbiological analysis, 2 L water samples were filtered through polycarbonate filters (pore size = 0.22 μm). Total DNA was



extracted from the water samples using the PowerSoil DNA Isolation Kit (MO BIO Laboratories, Carlsbad, CA, USA), according to the manufacturer's instructions. The quality of the extracted DNA was checked using agarose gel electrophoresis and the DNA was stored at -20°C . DNA concentrations were determined using a Qubit[®] 2.0 fluorometer. Microcosms were constructed, deployed, and analyzed using a modified version of the method of [Zhu et al. \(2020\)](#). Briefly, the V4 region of bacterial 16S rRNA was amplified using primer pair 515F and 806R. PCR amplicons were sequenced on an Illumina MiSeq platform at Beijing Biomarker Technologies, and sequences were analyzed using QIIME and UPARSE software with the default settings to obtain effective tags and operational taxonomic units (OTUs). The UPARSE pipeline was then used for taxonomic assignment at the 97% similarity level *via* Ribosomal Database Project Naïve Bayesian Classifier v.2.2, trained on the SILVA database (ver. 123), using a 0.8 confidence level as the cutoff. The Mothur package was used to calculate the abundance-based coverage estimator (ACE) and Shannon's diversity index.

2.4. n-Alkanes

To determine n-alkanes, the pH of the samples was adjusted to 2 and they were stored at 5°C until analysis. Methanol (10%) was added to the water samples before solid-phase extraction

(SPE). n-Alkanes were constructed, deployed, and analyzed using a modification of the approach of [Saim et al. \(2009\)](#). n-Alkanes were extracted using C18 SPE cartridges conditioned with 10 ml of methanol followed by 6 ml of ultrapure water at a rate of 1–2 ml/min. The cartridges were then dried under vacuum. A 4 L water sample was loaded into the SPE column at a rate of 6 ml/min. The cartridges were then dried under vacuum for 30 min. The n-alkanes were eluted using 2×3 ml of dichloromethane. The extract was blown down to 1 ml under a gentle flow of nitrogen, and then analyzed by gas chromatography–mass spectrometry (GC–MS, Agilent 7890A GC, 5975C MSD) in selected ion monitoring (SIM) modes with internal standards n-Alkanes, and Deuterated tetracosane was used as internal standard for quantifying. The analysis was carried out in Chongqing Key Laboratory of Karst Environment, School of Geographical Sciences, Southwest University.

3. Results

3.1. Aquifer geochemistry

Borehole B1 had Ca-SO_4 -type water with total dissolved substances (TDS) $> 1,000$ mg/L; borehole B2 to B6 had Ca-HCO_3 -type water with TDS $< 1,000$ mg/L. The groundwater

temperature varied from 23.4 to 27.1°C, i.e., did not vary markedly among boreholes; the pH ranged from 6.8 at B6 to 8.1 at B4. The d-excess also showed variation among wells, similar to the pH.

3.2. Taxonomic diversity

River water samples analyzed in this study was used to compare difference with groundwater samples. The coverage index of the sequenced samples ranged from 0.99 to 1.00; all values were >98%, indicating high reliability of the sequencing depth. The Shannon index was in the order B6 > B5 > B4 > B2 > R1 > B3 > B1, indicating a sequential decrease in microorganism diversity (Table 1). The OTUs obtained from the sequencing were analyzed taxonomically and represented 64 phyla, 200 classes, 370 orders, 540 families, 771 genera, and 814 species.

The distance measure used in CA (cluster analysis) was Pearson correlation, and the results are presented in a dendrogram (Figure 2). As shown in Figure 2, the groundwater in B3 and river water in R1 were grouped together, groundwater in B4 and B2 belonged to same cluster, and B5 and B1 were grouped together. In addition, the species-level composition and abundance in groundwater *Acinetobacter lwoffii* was present in all water samples, except for B6. Its abundance in the environment was 0.27% ~ 7.21% in well water samples and 15.8% in river water samples, indicating that *A. lwoffii* was the dominant bacterium species in the studied samples. *S. kujiense* was dominant in B2 and B6, with respective abundances of 3.38 and 9.28%; similar lower abundances of *Desulfovirga adipica* were also presented in B2 and B6. However, *S. kujiense* and *Desulfovirga adipica* were not found in the river water sample (R1). *Acinetobacter venetianus*, *Pseudomonas umsongensis*, *Pseudomonas viridiflava*, and *Roseomonas lacus* were also presented.

3.3. n-Alkanes

The total dissolved n-alkane concentrations varied from 11,586 to 18,400 ng/l among the wells. Groundwater from all wells

showed a unimodal distribution, with low-molecular-weight (LMW) n-alkanes having even numbers of carbons (n-C14 to n-C18) predominating; n-C16 was the dominant n-alkane (Figure 3). This indicates that the dissolved organic matter in the wells was of bacterial origin (Fang et al., 2014) and the dominant source of dissolved organic carbon in the aquifer is likely microbial primary production.

4. Discussion

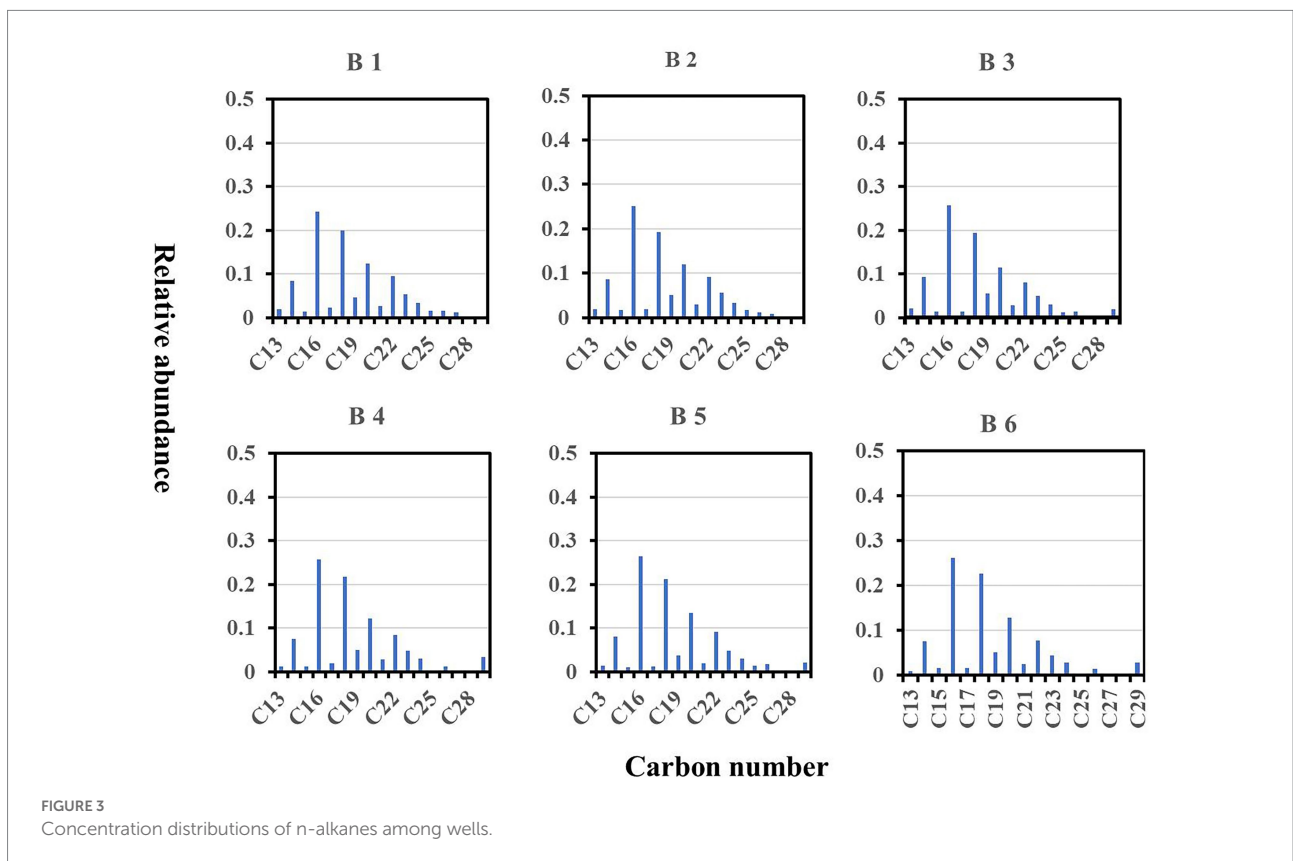
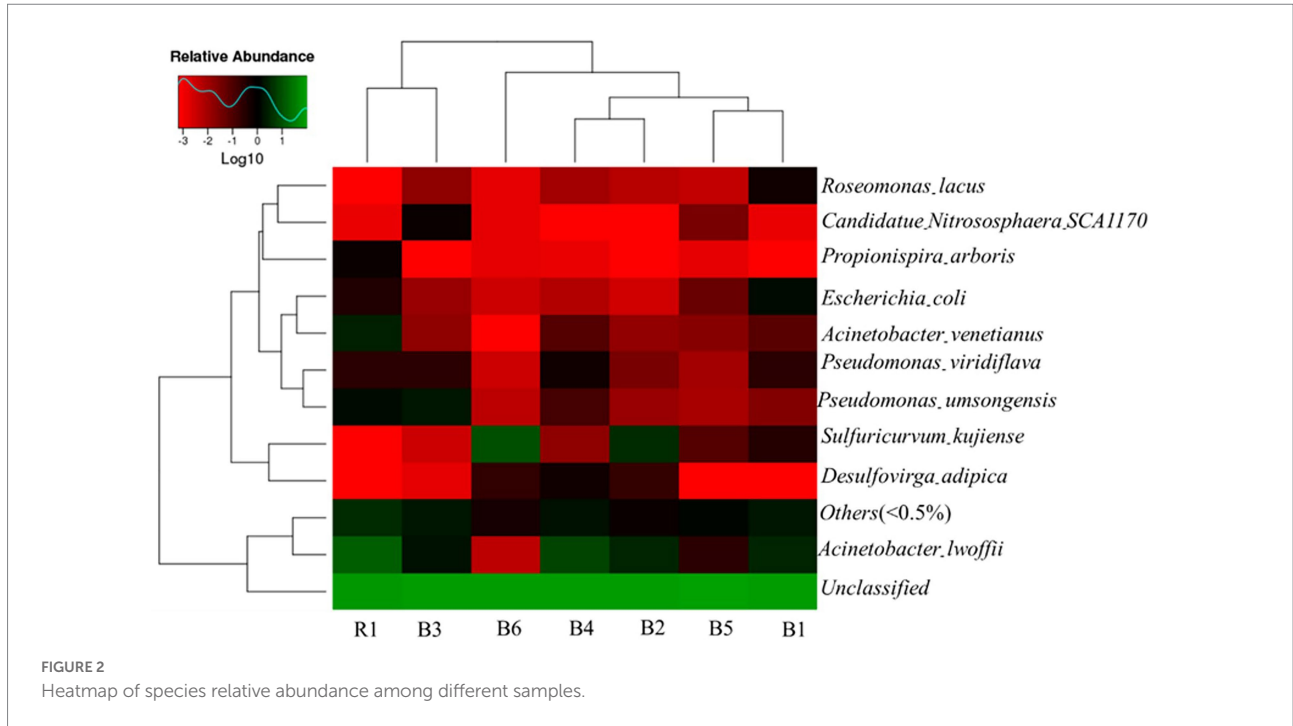
4.1. Hydrodynamic characteristics among different karst aquifer system

Heat carried by groundwater serves as a tracer to identify flow through fractures, and flow patterns in groundwater basins (Anderson, 2005), and the groundwater flow in the preponderance flow path interferes with the normal temperature distribution of the formation, and the information of groundwater seepage in the formation can be inferred from the anomaly of the temperature curve (Chi et al., 2020). In this study, six boreholes 'temperature-depth' profile were used to characterize the hydraulic properties of aquifers, the temperature gradient in B1, B2, B3, B4, B5, and B6 were 4.3, 1.7, 1.5, 0.6, 1.8, and 1.0°C/100 m, respectively (Figure 4). Among the selected boreholes, B1 belongs to non-karst aquifer and gypsum interlayer grows on it, which can also be reflected from the high SO₄²⁻ concentration in groundwater (Table 2). It also be found that lower temperature gradient was also corresponded to higher *k* values in karst aquifers (especially in B2, B3, B5 and B6).

In the karst aquifer system, there are groundwater migration channels such as pores, fissures, and cavities with large diameters. In areas where karst is not formed, rock mass is dense, and small pores are dominant, groundwater flow rate is very slow, even water-tight. It can be concluded that from borehole B2 to B6, karst aquifers are featured by vertical flow and have the characteristics of groundwater seepage. Especially, in the light of borehole profile description between wells (Supplementary Figure S1), the karst aquifer in B5 showed high permeability, karstification was well developed, and fissures and caves were found. By contrast, aquifer in B1 was not karst aquifer, and the vertical flow rate is slow. In addition, groundwater age estimation using tritium (³H) only provides semi-quantitative values (Brkic et al., 2016): <0.8 TU indicates sub-modern water (recharged prior to 1950s), 0.8 to ~4 TU indicates a mix of sub-modern and modern water, 5 to 15 TU indicates modern water (<5 to 10 years), 15–30 TU indicates some bomb tritium and > 30 TU indicates recharged occurred in the 1960s to 1970s. As shown in Table 2, B3 and B6 had ³H values higher than 5 TU, indicating modern water (< 5 to 10 years) in above aquifers; whereas ³H values in B2, B4 and B5 all higher than 0.8 TU and lower than 4 TU, showing a mix of sub-modern and modern water in above aquifers. And B1 showing ³H values lower than 2, which may

TABLE 1 Diversity and richness estimators for pyrosequence libraries.

Sample	Unique sequences	97% OTUs	Shannon	Coverage
R1	73,492	340	2.73	1.00
B1	69,975	1989	3.58	1.00
B2	76,178	1,084	3.98	1.00
B3	73,098	1769	3.94	0.99
B4	65,225	2,519	4.17	1.00
B5	74,911	1,081	4.99	1.00
B6	72,031	1,251	5.38	0.99



indicate sub-modern water in it. Hence, combined with the ‘temperature-depth’ profile characteristics and ³H values above in selected boreholes, it can conclude that karst aquifer

in borehole B1 belongs to regional flow, karst aquifers in borehole B3 and B6 perhaps belong to local flow, and karst aquifers in borehole B2, B4 and B5 maybe belong to

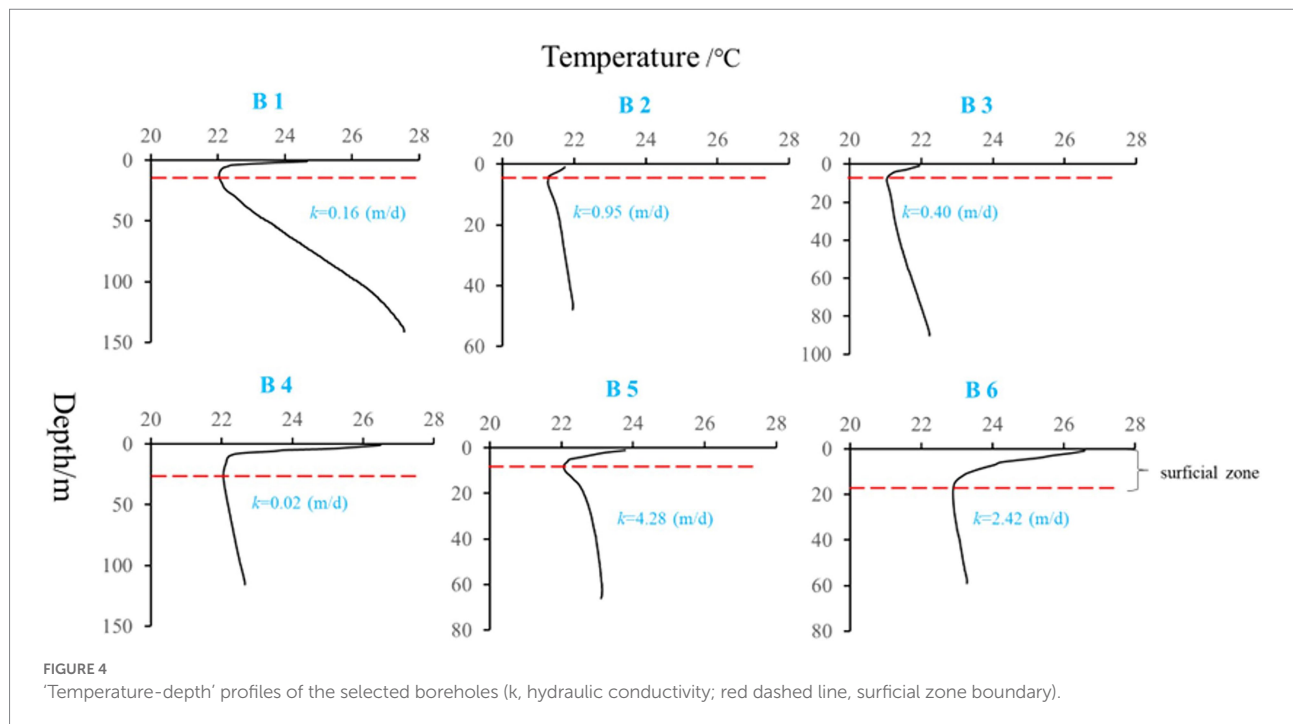


TABLE 2 Chemical and physical properties among different wells.

Item	River		Well				
	R1	B1	B2	B3	B4	B5	B6
TDS(mg/L)	437	2,652	499	377	164	304	409
DO(mg/L)	3.2	2.1	1.9	2.2	2.1	1.8	1.5
T(°C)	25	25.8	27.1	23.4	23.6	25.8	25.6
Ph	6.9	7.3	6.9	7.5	8.1	7.7	6.8
DOC(mg/L)	0.9	0.7	0.6	0.5	0.5	1	1.6
d-excess (%)	13.3	11.3	7.8	13.1	12.8	11.7	10.1
$\delta^{13}\text{C}_{\text{DIC}}$ (‰)	-	-8.19	-7.88	-8.09	-4.65	-7.88	-8.66
^3H (TU)	-	< 2	3.44	8.27	2.78	3.16	6.61
HCO_3^- (meq/L)	4	3	7.2	4	2.4	3.2	4.3
Cl^- (meq/L)	0.9	0.2	0.1	0.1	0	0.1	0.2
NO_3^- (meq/L)	1	BDL	0	0	0.1	0.1	BDL
SO_4^{2-} (meq/L)	0.4	42	0.3	0.5	0.2	0.5	0.6
K^+ (meq/L)	0.4	0.1	0	0	0	0	0.1
Na^{2+} (meq/L)	0.8	1.7	0.1	0	0	0	0.3
Cl^- (meq/L)	0.9	0.2	0.1	0.1	0	0.1	0.2
Ca^{2+} (meq/L)	4.7	17	1.8	4.3	0.3	3.9	4.4
Mg^{2+} (meq/L)	0.2	5.7	0.2	1.4	0.1	0.4	0.7

DO, dissolved oxygen; BDL, below detection limit; DOC, dissolved organic carbon; d-excess, deuterium excess; -, missing data.

intermediate flow. In addition, similar distribution of microbe species between river water and groundwater in B3 also support that groundwater in B3 was more potentially influenced by seepage, and which should belong to local flow.

4.2. Potential factors influencing microbe activities in selected karst aquifers

Principal Component Analysis (PCA) is based on the diagonalization of the correlation matrix, which can not only

point out associations between variables that can show the global coherence of the data set, but also it will evidence the participation of the individual chemical parameters in several influence factors (Helena et al., 2000), and help to explore the dominating factors in the geochemistry (Hu et al., 2013). In this study, PCA was performed to identify potential factors influencing microbe activities in selected karst aquifers, which is a common phenomenon in hydrochemistry.

In the PCA, the first three eigenvalues were greater than one and explained more than 88% of the variance (Table 3). The first principal component (PC1) accounted for more than 47.9% of the variance in the data and had high positive loadings for *A. lwoffii*, *A. venetianus*, *Escherichia coli*, *Propionispira arboris*, EC, DO, Cl^- , NO_3^- , K^+ , and Na^+ . In groundwater, *E. coli* and NO_3^- are usually from the input of effluent (Dougherty et al., 2009), while K^+ and Na^+ ions can result from agricultural fertilizer use in rural and suburban areas, as well as from livestock manure and sewer leakage (Liang et al., 2018). This indicates that *A. lwoffii*, *A. venetianus*, *E. coli*, and *P. arboris* were not from the internal environment of the karst aquifer.

The second principal component (PC2) accounted for more than 24.4% of the variance and had high loadings for *P. viridiflava*, pH, and d-excess (all positive) and *S. kujiense*, temperature, and HCO_3^- (all negative). *S. kujiense* is a parthenogenetic, anaerobic, chemoautotrophic sulfur-oxidizing bacterium, and temperature and pH control sulfur-oxidizing bacterium. This indicates that the HCO_3^- concentration increased with the density of *S. kujiense*.

The third principal component (PC3) accounted for more than 16.47% of the variance and had high loadings for *P. umsongensis*, *Candidatus Nitrososphaera SCA1170*, and SO_4^{2-} (all positive) and *D. adipica* (negative), and moderate loading for *R. lacus*. This indicates that the SO_4^{2-} concentration increased with the relative abundance of *Candidatus Nitrososphaera SCA1170* and *P. umsongensis*, but decreased with the relative abundance of *D. adipica*.

In this study, the length of the gradient in the first axis calculated by detrended correspondence analysis (DCA) was <3, which was 2.8 in our study, the redundancy analysis (RDA) model should be selected to evaluate the potential relationship between the distribution of microbe species and environmental parameters (Chen et al., 2015), but the *p* values of environmental factors in groundwater were all higher than 0.05, which can not be used to evaluate the potential relationship between the distribution of microbe species and environmental parameters in our study. Hence, the relationship between microbe species abundance and groundwater environmental factors in six selected boreholes was evaluated by multivariate analysis (Figure 5).

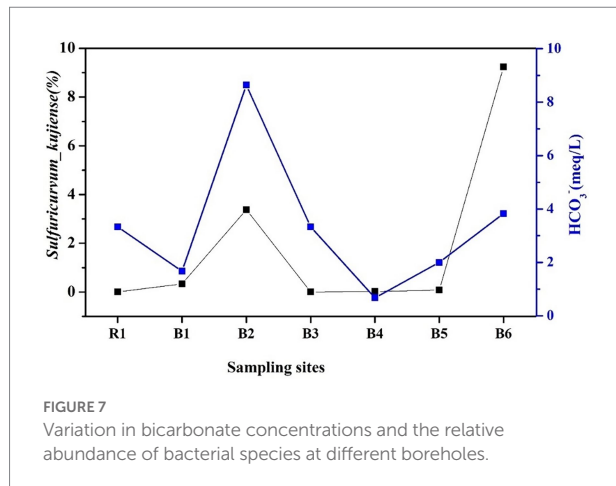
As shown in Figure 5, similar relationships were found between selected microbe species (*E. coli* and *R. lacus*) and groundwater environmental factors (K^+ , Na^+ , Ca^{2+} , Mg^{2+} , and $\text{SI}_{\text{dolomite}}$), indicating *E. coli* and *R. lacus* may produce influence on groundwater chemistry types. And also, *S. kujiense* showed higher positive relationship with HCO_3^- ($p < 0.05$), indicating the

TABLE 3 The main component load of bacterial species and their water physics and chemical parameters.

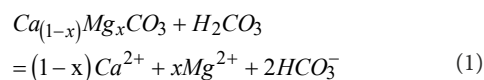
Items	PC 1	PC 2	PC 3
<i>Acinetobacter_lwoffii</i>	0.858	0.21	-0.338
<i>Acinetobacter_venetianus</i>	0.995	0.047	-0.064
<i>Candidatus_Nitrososphaera_SCA1170</i>	-0.243	0.39	0.881
<i>Desulfovira_adipica</i>	-0.423	0.256	-0.717
<i>Escherichia_coli</i>	0.995	0.041	-0.057
<i>Propionispira_arboris</i>	0.997	0.032	-0.046
<i>Pseudomonas_umsongensis</i>	0.452	0.432	0.752
<i>Pseudomonas_viridiflava</i>	0.032	0.819	-0.329
<i>Roseomonas_lacus</i>	-0.552	0.267	0.547
<i>Sulfuricurvum_kujiense</i>	-0.259	-0.868	-0.052
EC	0.645	-0.491	0.492
DO	0.943	0.258	0.024
Temperature	0.039	-0.971	-0.179
pH	-0.555	0.714	-0.316
DOC	0.547	-0.302	-0.209
d-excess	0.373	0.895	0.12
HCO_3^-	-0.03	-0.87	0.253
Cl^-	0.999	0.007	-0.031
NO_3^-	0.994	0.047	-0.09
SO_4^{2-}	0.118	0.009	0.85
K^+	0.995	-0.047	-0.052
Na^+	0.989	-0.092	-0.034
Eigenvalue	10.55	5.37	3.62
Total variance (%)	47.94	24.41	16.47
Cumulative variability (%)	47.94	72.35	88.82

abundance of *S. kujiense* in karst groundwater was an important factor that influencing HCO_3^- concentrations.

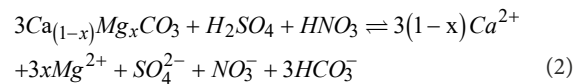
Because the HCO_3^- concentration increased with the density of *S. kujiense*. It is necessary to assess the solubility of carbonate minerals based on bulk aquifer fluid geochemistry before considering the potential for microbially mediated carbonate dissolution. By calculating the saturation index (SI), the equilibrium state of water with respect to a particular mineral phase can be determined, and which can also be used to distinguish the hydrogeochemical evolution as well as by identifying the geochemical reactions that control the water chemistry (Li et al., 2019a; Subba Rao et al., 2022). The saturation indexes of calcite, dolomite, and gypsum were calculated to interpret the hydrogeochemical processes in the six wells (Figure 5). The



processes. For instance, carbonic acid and anthropogenic acids (e.g., sulfuric and nitric acid) increase the dissolution of carbonate and HCO_3^- concentration in groundwater (Huang et al., 2017). Carbon isotopes in groundwater ($\delta^{13}\text{C}_{\text{DIC}}$) can be used to identify different acids affecting carbonate dissolution (Ali and Atekwana, 2011). In the study area, the rainwater was typically acidic, with a volume-weighted mean pH of 4.49 (Cao et al., 2009), which indicates that atmospheric CO_2 makes a negligible contribution to dissolved inorganic carbon (DIC). The DIC in the study area likely has two primary sources: the weathering of carbonate minerals and the dissolution of CO_2 in soil (Eq. 1).



Open-system carbonate weathering mediated solely by carbonic acid requires that the isotopic composition of DIC is continuously in equilibrium with the gaseous phase of a given pCO_2 , and that continuous isotopic exchange occurs between CO_2 and the aqueous solution. Thus, $\delta^{13}\text{C}_{\text{DIC}}$ is controlled mainly by the hydrolysis of CO_2 in soil (Jiang et al., 2013; Huang et al., 2017). Therefore, the $\delta^{13}\text{C}_{\text{DIC}}$ in karst groundwater under open-system conditions should be around -14% (i.e., -23% plus $+9\%$; Jiang et al., 2013). In a closed-system, the amount of soil-derived CO_2 decreases gradually over time during carbonic acid-driven carbonate dissolution; as the carbon in our groundwater samples was produced from carbonate and soil-derived CO_2 in approximately equal amounts, the $\delta^{13}\text{C}_{\text{DIC}}$ should approach a value of -11.5% [i.e., $0.5 \times (-23\% + 0)$] (Jiang et al., 2013). When carbonate dissolution is facilitated by other acids (e.g., sulfuric, nitric, or organic acid), all DIC is derived from non-carbonic acid carbonate dissolution (Eq. 2), so it has a $\delta^{13}\text{C}$ value (0%) identical to that of the constituent carbonate minerals (Li et al., 2008; Jiang et al., 2013).



For the groundwater analyzed, the $\delta^{13}\text{C}_{\text{DIC}}$ values were in the range -8.66% to -4.65% with a mean value of -7.56% , which is significantly more positive than -11.5% (Table 2). This suggests that carbonate dissolution in the study area was likely facilitated by additional acids. Because groundwater recharge areas have vast areas of fertile agricultural land, higher levels of domestic sewage and nitrogenous fertilizers percolate through the topsoil and enter the karst aquifers, which can increase carbonate dissolution (Yamanaka, 2012). The larger range of $\delta^{13}\text{C}_{\text{DIC}}$ values is strongly related to enhanced carbonate dissolution by nitric and sulfuric acids.

5. Conclusion

The main conclusion of this study is that carbonate dissolution in the deep karst aquifer was potentially influenced by microbial activity (e.g., *S. kujense*) and the input of anthropogenic acids, as evidenced by significantly more positive $\delta^{13}\text{C}_{\text{DIC}}$ values. This ultimately changes the hydraulic properties of karst aquifers. However, more studies are needed to quantify the effect of microbial activity on carbonate dissolution in the karst aquifer.

Data availability statement

The data presented in the study are deposited in the NCBI repository, accession number PRJNA917210.

Author contributions

ZL wrote the manuscript. SL, ZW, RL, and ZY performed the data collection and the bioinformatic analysis. JC and LG conceived the idea and supervised the work. YS performed the lipids biomarker analysis. All authors contributed to the article and approved the submitted version.

Funding

This work was financially supported by Natural Science Foundation of Guangdong Province of China (2021A1515110505), Open Funding Project of the Key Laboratory of Groundwater Sciences and Engineering, Ministry of Natural Resources (SK202102), National Natural Science Foundation of China (41961144027 and 41771027), China Postdoctoral Science Foundation (2021M703657), Scientific and Technological

Innovation Project of the Water Sciences Department of Guangdong Province (2020–09), and Asia-Pacific Network for Global Change Research (APN; CRRP2019-09MY-Onodera).

Acknowledgments

We thank Lixiang Cao for the help with manuscript formatting the valuable technical help.

Conflict of interest

The authors declare that the research was conducted in the absence of any commercial or financial relationships that could be construed as a potential conflict of interest.

References

- Ali, H. N., and Atekwana, E. A. (2011). The effect of sulfuric acid neutralization on carbonate and stable carbon isotope evolution of shallow groundwater. *Chem. Geol.* 284, 217–228. doi: 10.1016/j.chemgeo.2011.02.023
- Anderson, M. P. (2005). Heat as a ground water tracer. *Ground Water* 43, 951–968. doi: 10.1111/j.1745-6584.2005.00052.x
- Brkic, Z., Briski, M., and Markovic, T. (2016). Use of hydrochemistry and isotopes for improving the knowledge of groundwater flow in a semiconfined aquifer system of the Eastern Slavonia (Croatia). *Catena* 142, 153–165. doi: 10.1016/j.catena.2016.03.010
- Cao, Y.-Z., Wang, S., Zhang, G., Luo, J., and Lu, S. (2009). Chemical characteristics of karst water system using temperature tracer technique. *Atmos. Res.* 94, 462–469. doi: 10.1016/j.atmosres.2009.07.004
- Chen, H., Liu, S., Xu, X. R., Zhou, G. J., Liu, S. S., Yue, W. Z., et al. (2015). Antibiotics in the coastal environment of the Hailing Bay region, South China Sea: spatial distribution, source analysis and ecological risks. *Mar. Pollut. Bull.* 95, 365–373. doi: 10.1016/j.marpolbul.2015.04.025
- Chi, G., Xing, L., Xing, X., Li, C., and Dong, F. (2020). Seepage characteristics of karst water system using temperature tracer technique. *Earth Space Sci.* 7:e2019EA000712. doi: 10.1029/2019EA000712
- Corbella, M., and Ibáñez, C. A. (2003). Role of fluid mixing in deep dissolution of carbonates. *Geol. Acta* 1, 305–313. doi: 10.1344/105.000001618
- Dansgaard, W. (1964). Stable isotopes in precipitation. 16, 436–468. doi: 10.1111/j.2153-3490.1964.tb00181.x
- Derrien, M., Yang, L., and Hur, J. (2017). Lipid biomarkers and spectroscopic indices for identifying organic matter sources in aquatic environments: a review. *Water Res.* 112, 58–71. doi: 10.1016/j.watres.2017.01.023
- Dougherty, M. C., Thevathasan, N. V., Gordon, A. M., Lee, H., and Kort, J. (2009). Nitrate and *Escherichia coli* NAR analysis in tile drain effluent from a mixed tree intercrop and monocrop system. *Agric. Ecosyst. Environ.* 131, 77–84. doi: 10.1016/j.agee.2008.09.011
- Engel, A. S., Porter, M. L., Stern, L. A., Quinlan, S., and Bennett, P. C. (2004a). Bacterial diversity and ecosystem function of filamentous microbial mats from aphotic (cave) sulfidic springs dominated by chemolithoautotrophic “Epsilonproteobacteria”. *FEMS Microbiol. Ecol.* 51, 31–53. doi: 10.1016/j.femsec.2004.07.004
- Engel, A. S., and Randall, K. W. (2011). Experimental evidence for microbially mediated carbonate dissolution from the saline water zone of the Edwards aquifer, Central Texas. *Geomicrobiol. J.* 28, 313–327. doi: 10.1080/01490451.2010.500197
- Engel, A. S., Stern, L. A., and Bennett, P. C. (2004b). Microbial contributions to cave formation: new insights into sulfuric acid speleogenesis. *Geology* 32, 369–372. doi: 10.1130/G20288.1
- Fang, J., Wu, F., Xiong, Y., Li, F., du, X., An, D., et al. (2014). Source characterization of sedimentary organic matter using molecular and stable carbon isotopic composition of n-alkanes and fatty acids in sediment core from Lake Dianchi, China. *Sci. Total Environ.* 473–474, 410–421. doi: 10.1016/j.scitotenv.2013.10.066
- Ford, D., and Williams, P. (2007). Dissolution: chemical and kinetic behaviour of the karst rocks. *Karst Hydrogeol. Geomorphol.* 3, 39–76. doi: 10.1002/9781118684986.ch3
- Goldscheider, N., and Drew, D. (2007). *Methods in karst hydrogeology*. London: CRC Press.
- Goldscheider, N., Hunkeler, D., and Rossi, P. (2006). Review: microbial bioceneses in pristine aquifers and an assessment of investigative methods. *Hydrogeol. J.* 14, 926–941. doi: 10.1007/s10040-005-0009-9
- Gray, C. J., and Engel, A. S. (2013). Microbial diversity and impact on carbonate geochemistry across a changing geochemical gradient in a karst aquifer. *ISME J.* 7, 325–337. doi: 10.1038/ismej.2012.105
- Helena, B., Pardo, R., Vega, M., Barrado, E., Fernandez, J. M., and Fernandez, L. (2000). Temporal evolution of groundwater composition in an alluvial aquifer (Pisuergra River, Spain) by principal component analysis. *Water Res.* 34, 807–816. doi: 10.1016/S0043-1354(99)00225-0
- Hu, S., Luo, T., and Jing, C. (2013). Principal component analysis of fluoride geochemistry of groundwater in Shanxi and Inner Mongolia, China. *J. Geochem. Explor.* 135, 124–129. doi: 10.1016/j.gexplo.2012.08.013
- Huang, Q.-B., Qin, X.-Q., Liu, P.-Y., Zhang, L.-K., and Su, C.-T. (2017). Impact of sulfuric and nitric acids on carbonate dissolution, and the associated deficit of CO₂ uptake in the upper-middle reaches of the Wujiang River, China. *J. Contam. Hydrol.* 203, 18–27. doi: 10.1016/j.jconhyd.2017.05.006
- Jiang, Y., Hu, Y., and Schirmer, M. (2013). Biogeochemical controls on daily cycling of hydrochemistry and $\delta^{13}\text{C}$ of dissolved inorganic carbon in a karst spring-fed pool. *J. Hydrol.* 478, 157–168. doi: 10.1016/j.jhydrol.2012.12.001
- Li, S.-L., Calmels, D., Han, G., Gaillardet, J., and Liu, C.-Q. (2008). Sulfuric acid as an agent of carbonate weathering constrained by $\delta^{13}\text{C}$ DIC: examples from Southwest China. *Earth Planet. Sci. Lett.* 270, 189–199. doi: 10.1016/j.epsl.2008.02.039
- Li, S., Dong, L., Chen, J., Li, R., Yang, Z., and Liang, Z. (2019b). Vertical groundwater flux estimation from borehole temperature profiles by a numerical model, RFLUX. *Hydrol. Process.* 33, 1542–1552. doi: 10.1002/hyp.13420
- Li, P., He, X., and Guo, W. (2019a). Spatial groundwater quality and potential health risks due to nitrate ingestion through drinking water: a case study in Yan'an City on the Loess Plateau of Northwest China. *Hum. Ecol. Risk Assess. Int. J.* 25, 11–31. doi: 10.1080/10807039.2018.1553612
- Liang, Z., Chen, J., Jiang, T., Li, K., Gao, L., Wang, Z., et al. (2018). Identification of the dominant hydrogeochemical processes and characterization of potential contaminants in groundwater in Qingyuan, China, by multivariate statistical analysis. *RSC Adv.* 8, 33243–33255. doi: 10.1039/C8RA06051G
- Liu, K., Qiao, X., Li, B., Sun, Y., Li, Z., and Pu, C. (2016). Characteristics of deuterium excess parameters for geothermal water in Beijing. *Environ. Earth Sci.* 75:1485. doi: 10.1007/s12665-016-6285-y
- Liu, J., Zhao, Y., Tan, T., Zhang, L., Zhu, S., and Xu, F. (2022). Evolution and modeling of mine water inflow and hazard characteristics in southern coalfields of China: a case of Meitanba mine. *Int. J. Min. Sci. Technol.* 32, 513–524. doi: 10.1016/j.ijmst.2022.04.001

Publisher's note

All claims expressed in this article are solely those of the authors and do not necessarily represent those of their affiliated organizations, or those of the publisher, the editors and the reviewers. Any product that may be evaluated in this article, or claim that may be made by its manufacturer, is not guaranteed or endorsed by the publisher.

Supplementary material

The Supplementary material for this article can be found online at: <https://www.frontiersin.org/articles/10.3389/fmicb.2022.1054295/full#supplementary-material>

- Loaiciga, H. A. (2009). Long-term climatic change and sustainable ground water resources management. *Environ. Res. Lett.* 4:035004. doi: 10.1088/1748-9326/4/3/035004
- Macalady, J. L., Lyon, E. H., Koffman, B., Albertson, L. K., Meyer, K., Galdenzi, S., et al. (2006). Dominant microbial populations in limestone-corroding stream biofilms, Frasassi Cave System, Italy. *Appl. Environ. Microbiol.* 72, 5596–5609. doi: 10.1128/AEM.00715-06
- MacInnis, I. N., and Brantley, S. L. (1992). The role of dislocations and surface morphology in calcite dissolution. *Geochim. Cosmochim. Acta* 56, 1113–1126. doi: 10.1016/0016-7037(92)90049-O
- Parsons, M. L. (1970). Groundwater thermal regime in a glacial complex. *Water Resour. Res.* 6, 1701–1720. doi: 10.1029/WR006i006p01701
- Saim, N., Osman, R., Sari Abg Spian, D. R., Jaafar, M. Z., Juahir, H., Abdullah, M. P., et al. (2009). Chemometric approach to validating faecal sterols as source tracer for faecal contamination in water. *Water Res.* 43, 5023–5030. doi: 10.1016/j.watres.2009.08.052
- Sjöberg, E. L., and Rickard, D. T. (1984). Calcite dissolution kinetics: surface speciation and the origin of the variable pH dependence. *Chem. Geol.* 42, 119–136. doi: 10.1016/0009-2541(84)90009-3
- Subba Rao, N., Dinakar, A., and Sun, L. (2022). Estimation of groundwater pollution levels and specific ionic sources in the groundwater, using a comprehensive approach of geochemical ratios, pollution index of groundwater, unmix model and land use/land cover - a case study. *J. Contam. Hydrol.* 248:103990. doi: 10.1016/j.jconhyd.2022.103990
- Wang, Z., Guo, X., Kuang, Y., Chen, Q., Luo, M., and Zhou, H. (2022). Recharge sources and hydrogeochemical evolution of groundwater in a heterogeneous karst water system in Hubei Province, Central China. *Appl. Geochem.* 136:105165. doi: 10.1016/j.apgeochem.2021.105165
- Yamanaka, M. (2012). Contributions of C3/C4 organic materials and carbonate rock to dissolved inorganic carbon in a karst groundwater system on Miyakojima Island, southwestern Japan. *J. Hydrol.* 412-413, 151–169. doi: 10.1016/j.jhydrol.2011.07.046
- Zhao, Y., Liu, Q., Zhang, C., Liao, J., Lin, H., and Wang, Y. (2021). Coupled seepage-damage effect in fractured rock masses: model development and a case study. *Int. J. Rock Mech. Min. Sci.* 144:104822. doi: 10.1016/j.ijrmms.2021.104822
- Zhao, Y., Zhang, L., Liao, J., Wang, W., Liu, Q., and Tang, L. (2020). Experimental study of fracture toughness and subcritical crack growth of three rocks under different environments. *Int. J. Geomech.* 20:04020128. doi: 10.1061/(ASCE)GM.1943-5622.0001779
- Zhu, A., Yang, Z., Liang, Z., Gao, L., Li, R., Hou, L., et al. (2020). Integrating hydrochemical and biological approaches to investigate the surface water and groundwater interactions in the hyporheic zone of the Liuxi River basin, southern China. *J. Hydrol.* 583:124622. doi: 10.1016/j.jhydrol.2020.124622